A NEW METHOD FOR DESIGN AND CONTROL OF HAPTIC INTERFACES FOR DISPLAY OF RIGID SURFACES

Scott L. Springer and Nicola J. Ferrier

University of Wisconsin – Madison, Department of Mechanical Engineering
1513 University Avenue
Madison, Wisconsin 53706
springer@idcnet.com, ferrier@engr.wisc.edu

Abstract

This paper addresses the often-cited problems associated with haptic display of rigid bodies or "virtual walls". Traditional haptic interfaces employ an actuator directly coupled to the human operator that provides a force proportional to wall penetration distance and velocity. A new paradigm for design and control of haptic displays is proposed that utilizes a de-coupled actuator and pre-contact distance sensing to improve stability and response performance. Dynamic models of real human/rigid body contact and prior haptic display models are developed and compared with the proposed method. Errors in the force and energy transfer are identified and associated with virtual wall penetration distance, required in traditional virtual wall haptic models. Results of the simulation of the dynamic models are presented, identifying system force response errors attributable to delay, wall penetration, wall model spring constant, and wall model damping constants.

1. Introduction

One key area of haptic simulation is the ability to present to the operator the sensation of initial contact with rigid objects or virtual walls. Many researchers have reported undesirable vibration when attempting to simulate stiff surfaces. Kazerooni (1993) analyzed the stability of a position controlled (joystick type) haptic interface, coupled to the human operator. The time delay between input force, sensed at the controller, and hand controller position response results in oscillatory hand controller motion due to "limit cycle instability". To address this problem, Kazerooni recommends a sampling time smaller than 0.003 seconds. Salcudean and Vlaar (1994) provide a typical model of the stiff wall component of a hand held joystick interacting with a stiff wall as:

$$f_k = -k_p\, x_{k-1} \; -(k_v/T)\,(x_{k-1} - x_{k-2}) \qquad (1)$$

when implemented in a discrete time PD controller, using a first order finite difference approximation of the velocity term. In EQ. (1) k_p is the potential energy constant and k_v is the damping (velocity dependant) constant. Salcudean and Vlaar (1994) show by examination of the roots of the closed loop characteristic polynomial, fundamental limitations on the achievable virtual stiffness and damping. For m = 0.7 kg, 1/T = 200 Hz, the maximum k_p is 3900 N/m, while k_v assumes a maximum value of 60 N/(m/s). They further comment that such an implementation would lead to a "marginally stable system", and recommend that a "braking pulse" be implemented providing a very high damping upon wall penetration to increase perceived stiffness of virtual walls.

Love and Book (1995) also analyze the contact stability of virtual walls utilizing Jury's test to evaluate the bounds of the parameters of the system's characteristic equation. Their analysis shows that stability can be lost by increasing stiffness for a given sampling rate and damping, or can also be lost by employing a simulation damping that is either too small or too large for a given stiffness and sampling rate. They also show that for a given damping and stiffness, increasing the sampling rate can restore stability of contact with virtual walls. Colgate, et.al.(1993) also analyze the stability of contact with virtual walls represented by EQ. (1) focusing on maintaining stability, by maintaining passivity of the wall.

Ellis, et.al. (1997) also studied the rendering of contact, particularly with stiff surfaces and developed numerical methods to reduce the error in force values presented to the operator. Their method primarily consists of estimation of the force to be presented based on the slope of the force/time curve between the prior two force values. The analysis consists of lagrangian dynamic modeling of the haptic interface. In the present analysis, the general analysis approach of Ellis et.al. is followed, with the exception that this analysis considers the operator, in combination with a real wall, a traditional virtual wall simulation, and the wall simulation rendered by the proposed de-coupled actuator/pre-contact distance sensing control algorithm.

2. Description of Proposed Method

The new method of design and control of haptic interfaces to address the challenge of high-speed stable display of rigid surfaces utilizes a de-coupled actuator in combination with feed-forward control (DECAFF). The feed forward control is based

on sensed (in the case of tele-robotic slave entities) or calculated (in the case of virtual slave entities) distances between the slave and any objects in close proximity to it. The proposed method calls for an actuator that is de-coupled from the human operator, and assumes a position of non-contact when the slave entity is not in contact with any neighboring objects. As the slave entity is brought within the vicinity of objects within the slave environment, the distance between the slave and a nearby object is sensed (or calculated) and used to control the actuator to assume a proportionate position of proximity to contact with the human operator. Thus further motion of the operator to cause the slave to move into contact with the neighboring object results in operator interference with the actuator. This method permits representation of extremely large changes in force experienced by the operator to occur over very short time spans. One embodiment of such an interface initially conceived for facilitation of haptic display in a VR-CAD application (Springer and Gadh, 1996, 1997), is under development at the University of Wisconsin-Madison. Recognizing the difficulty in haptic presentation of rigid bodies using prior haptic interface design and control methods, it was discovered during experimentation that a separation between the operator and the actuator, which could selectively and controllably be eliminated, permits the development of a device that provides several desirable features. The method not only provides a very high degree of transparency (while not in contact with slave environment objects), but also permits an extremely crisp sensation of initial contact, without chatter or disturbing oscillations, commonly reported in the literature.

This device is designed to provide force resisting finger bend during grasping operations. Each finger is represented by a single degree of freedom, with the motion of each fingertip being transmitted via hand mounted planar linkages and sheathed cable to a remote replicated finger as shown schematically in FIG. 1. The replicated finger consists of a linear link, pivotally mounted to a potentiometer, which measures finger bend as a single variable. A contact drum is mounted in the plane of replicated finger motion, driven by a DC motor, controlled such that the contact drum may selectively be brought into a position of contact with the replicated finger. The contact drum may be controlled either by position, to display initial contact with rigid bodies, or by force to display variable force of contact during interaction with non-rigid bodies. For representation of virtual walls, the distance between the (slave) virtual fingertip and neighboring objects is calculated within the virtual environment. This pre-contact distance information is used by the haptic interface controller to appropriately control the position of the contact drum such that further retraction of the finger will result in replicated finger/contact drum interference, resulting in restricted grasp motion of the operator's finger(s). During interaction with non-rigid objects, the force of contact between the contact drum and the replicated finger is controlled by a PWM motor torque control algorithm, delivering the operator a wide range of forces, consistent with the virtual reality simulation. Springer (1998), and Springer and Ferrier (1999) give a detailed description of the system design and DECAFFF control algorithm.

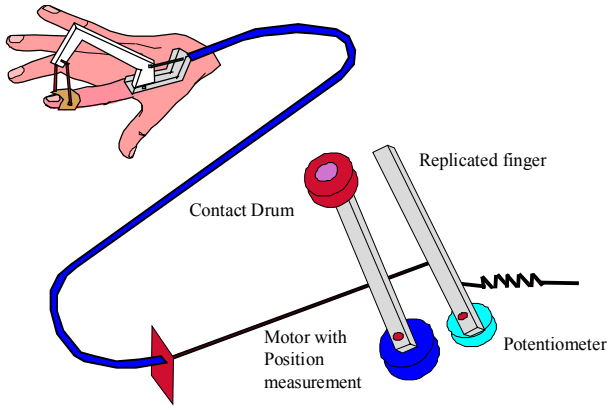

Figure 1 - Schematic of Proposed Design

The proposed haptic interface design and control paradigm in this research advances the state of the art in the haptic rendering of contact with stiff surfaces. This is done by reducing the time delay between slave finger/object contact and force display to the operator, thereby reducing slave position errors, and permitting more rapid movement and precise control during tele-manipulation, and permitting display of rigid virtual surfaces, without required surface penetration of prior approaches (eg. EQ. (1)). The slave position error is reduced by including a feed forward control variable, measurement of the distance to contact, before contact between the slave and the object has occurred. The use of a distance sensor to better control contact between a robotic slave and a grasped object, was proposed by Li (1996), but for application to multi-phase control, not human controlled tele-manipulation. We have found no articles in the literature describing a distance before contact control strategy for haptic display for a virtual slave application domain. A de-coupled actuator is proposed, that operates on the distance information to properly control the location of the master contact sensed by the operator, before the actual contact has occurred.

3. Dynamic Modeling of Rigid Body Contact

To effectively analyze the dynamics of contact, traditional mass/spring/damper models are considered for the following cases: (i) contact between a real (human) finger and a real physical wall, (ii) contact simulation modeling provided by traditional haptic displays, and (iii) contact simulation modeling provided by the DECAFF haptic display of the present research. For each of the three models, the force experienced by the operator and the energy transfer is considered in evaluating how closely simulation cases (ii) and (iii) resemble real contact of case (i).

3.1 Human Finger Contact with Real Wall

First considering the case of real contact between a human finger (or other body part) and a real wall, we model the finger as a mass, spring, damper system that interacts with a non-movable wall entity. The initial single DOF, linear displacement model is later

generalized to a multi-DOF, spatial model. The finger mass is denoted by m_f, while the spring rate and damping are denoted by k_f, and c_f, respectively, as shown in FIG. 2. The finger initially in a position just before contact, at time t_1, has a velocity v_1, and after contact (force transients have settled to a steady state value) at time t_2 the velocity is zero. Considering F(t) as the force felt by the person's sensory system and by application of Newton's second law we have the following equation of motion.

$$F(t) = m_f\, x''_f - c_f\, x'_f - k_f\, x_f \qquad (2)$$

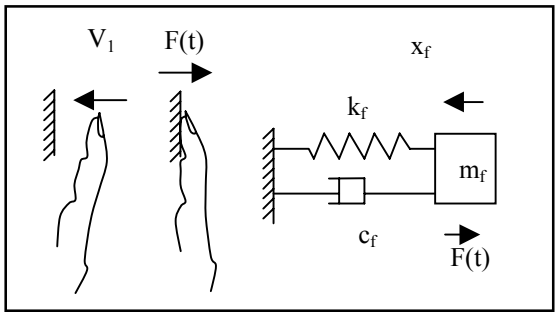

Figure 2 - Human Finger Contacting Real Wall

Where F(t) is the force of contact *experienced* by the person (of opposite direction as that applied by the person), m_f is the finger mass, c_f is the finger damping coefficient, k_f is the finger spring constant, x''_f, x'_f, and x_f are the acceleration, velocity, and position of the finger. The force just before contact will be given by the product of the mass and acceleration, while after contact, the force will be given by:

$$F(t_2) = m_f\, x''_f(t_2) - c_f\, x'_f(t_2) - k_f\, x_f(t_2) \qquad (3)$$

However at time t_2, the contact phase (of highly transient forces) is complete and the force has settled to a steady state value, resulting in an acceleration and velocity that are approximately equal to zero, yielding a final force of:

$$F(t_2) = -kx_f(t_2) \qquad (4)$$

In evaluating this force, first we consider the magnitude of x_2 which is of a small value due to the limited deflection of the fingertip touch pad (on the order of 4 mm). Secondly, the k value of the finger has been shown by others (Hajian and Howe, 1994 and Karson and Srinivasan, 1995) to assume a value proportional to the force applied. Thus, when the subject applies a small force to the wall at time t_2, following the initial contact phase k_f is also very small. A small force after the contact phase is most pronounced when subjects "tap" a wall, as shown in force time plots of Lawrence, et. al. (1996). Should the subject apply a high force after contact, the finger deflection remains relatively constant, and thus the k_f value increases proportionately. When we consider an energy balance between time (t_1) and time (t_2), we have:

$$E(t_1) = E(t_2) - U_{1\text{-}2} \qquad (5)$$

The energy of time (t_1) in EQ. (5) is completely kinetic, while that of time (t_2) is completely potential, and the work done between time (t_1) and time (t_2) is that absorbed by the damping of the human finger. Substitution of the appropriate terms into EQ. (5) yields:

$$(1/2)mx'(t_1)^2 = (1/2)kx(t_2)^2 + c(1/2)(x'(t_1) - x'(t_2))\, x(t_2) \qquad (6)$$

Again upon evaluation of the terms, we find that if the subject maintains a low contact force after initial contact, k_f is small and $x(t_2)$ is small, from which we can conclude (assuming a high initial velocity) that $U_{1\text{-}2}$ is large, or most of the kinetic energy of the finger is absorbed by the internal damping in the finger. After the contact phase with a real wall $x'(t_2)$, the final velocity is zero as the force has settled to a steady state value.

3.2 Contact Simulation of Traditional Haptic Displays

Secondly we consider a two mass, spring damper system as shown in FIG. 3, as a model of the typical simulation of contact between virtual finger and a virtual wall, or contact between a slave manipulator and a rigid body, as felt by the operator. The model includes a simulation mass, spring and damper, and a finger mass, spring and damper, as well as positional changes for each mass, denoted as x_s, and x_f, respectively. Utilizing a lumped parameter model (Norton, 1999), the dynamic system can be evaluated by the model given in FIG. 3. For this system, the equation of motion is as follows:

$$F(t) = mx_{f+s}'' - c_{eq}x_{f+s}' - k_{eq}x_{f+s} \qquad (7)$$

Where

$$c_{eq} = (c_s\, c_f) / (c_s + c_f) \text{ and } k_{eq} = (k_s\, k_f) / (k_s + k_f) \qquad (8)$$

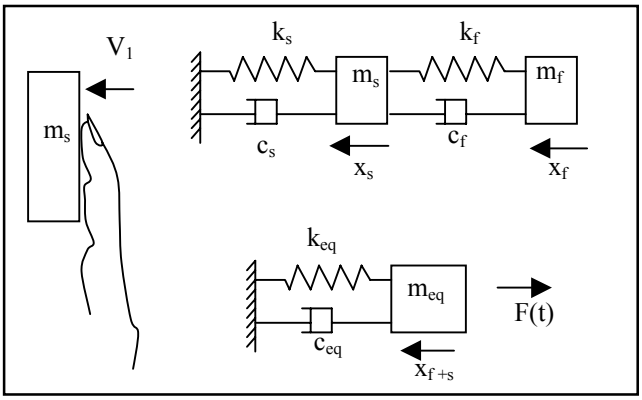

Figure 3 - Finger Contacting Simulated Wall (Traditional)

Both the equivalent damping coefficient and the equivalent spring constant in EQ. (7) and EQ. (8) assume a value close to the smaller of the two input terms, for wide variation between the finger and the simulation. Thus if k_f is very small and k_s is very large, k_{eq} will be approximated by k_f, as is done for the typical

wall model. Similar results hold for the effective damping. In evaluating the force and the energy balance as was done for the actual finger wall model, we see that the both the force and the energy at time (t_2) is higher for the simulated wall, since the magnitude of $x_{s+f}(t_2)$ is always greater than $x_f(t_2)$. Assuming the simulation at time (t_2) has stopped penetration motion and the force has reached a stable steady state value, and thus the velocity and acceleration are zero, the force value for large simulation stiffness k_s (typically implemented in a virtual wall model) is:

$$\text{For large } k_s \,(\, k_s >> k_f \,,\, k_{eq} = k_f) \quad F(t_2) = -k_f\, x_{f+s}(t_2) \qquad (9)$$

If we assume that finger deflection x_f for the simulation is approximately equal to x_f for the real wall, the error in steady state force magnitude is then given by the difference between the simulation force and the real wall contact force as:

$$F(t_2)_{sim} - F(t_2)_{real} = -k_f\, x_{f+s}(t_2) - k_f\, x_f(t_2) = -k_f\, x_s(t_2) \qquad (10)$$

When $x_f(t_2)_{real}$ is equal to $x_f(t_2)_{sim}$ and because $x_{f+s}(t_2)$ is equal to $x_f(t_2) + x_s(t_2)$, the error reduces to $-k_f\, x_s(t_2)$. Indicating that the error magnitude always increases with position error, due to the simulation wall penetration distance. In a haptic device simulation there are delays in display of the force, which we can divide into two categories: (i) a delay for the slave to assume the master position (δ_p), and (ii) the delay for the force determined at the slave to be displayed at the master (δ_f). It can be shown that the force F(t) at the master is delayed from the position of the master by the sum of these terms ($\delta_p + \delta_f$) or formally stated as:

$$F(t)_{master} = f\,\{\, P_{master}(t - \delta_p - \delta_f)\} \qquad (11)$$

Because the forces sensed by a person contacting a real wall are processed in a very small time, and the forces sensed when contacting a simulated wall are processed with a delay indicated by EQ. (11), the force magnitudes of a simulation also have a delay effect in error. The magnitude of this error is most pronounced during periods of highly transient forces as would appear between time t_1 and t_2 as defined above. Further, the penetration distance achieved while the force display is of zero magnitude during the delay of initial contact is directly proportional to the time delay and finger initial velocity. The above discussion clearly demonstrates that errors in the force felt by the operator are directly related to time delays in the haptic interface and penetration distance into the virtual wall (x_s). We find similar results upon consideration of the energy balance as was done for the real wall. For the typical case where the simulation damping and stiffness are significantly higher than that of the finger, we have:

$$E = (1/2)mx'(t_1)^2 =$$

$$(1/2)\, k\, x\,(t_2)^2 + c\,(1/2)\,[x'(t_1) - x'(t_2)]\, x\,(t_2) \qquad (12)$$

Which at time (t_2) yields a difference of potential energy of:

$$E(t_2)_{sim} - E(t_2)_{real} = (1/2)k_{eq}\, x_{f+s}(t_2)^2 - [(1/2)k_f\, x_f(t_2)^2] \qquad (13)$$

And yields a difference of damping energy of:

$$U_{1\text{-}2sim} - U_{1\text{-}2real} =$$

$$c_{eq}\,(1/2)\, x'(t_1)\; x_{f+s}(t_2) - [c_f\,(1/2)x'(t_1)\, x_f(t_2)] \qquad (14)$$

Combining EQ. (12) and EQ. (13) the total energy difference is:

$$= (1/2)k_f\,[x_f(t_2) + x_s(t_2)]^2 + c_f\,(1/2)x'(t_1)[x_f(t_2) + x_s(t_2)]$$

$$- [(1/2)k_f\, x_f\,(t_2)^2 + c_f\,(1/2)x'(t_1)x_f\,(t_2)] \qquad (14)$$

for $k_s >> k_f$, and $c_s >> c_f$, which reduces to:

$$= k_f\, x_s(t_2)\, x_f(t_2) + (1/2)\, k_f\, x_s(t_2)^2 + c_f\,(1/2)\, x'(t_1)\, x_s\,(t_2) \qquad (15)$$

This shows that the energy difference between a simulation and real wall (error) assumes a value increasing quadratically in simulation penetration distance $x_s(t_2)$, which upon real wall contact would be zero. The penetration distance depends on the system bandwidth, and is a result of both a time delay between the time of virtual hand crossing the wall edge and force output of EQ. (11), and the traditional wall dynamic model described in EQ. (1). A force and energy of an excess magnitude would be consistent with the typical description of the feeling of a virtual wall as "lively' or "active" (Colgate et. al., 1993). To increase the accuracy, the sampling period can be decreased (subject to computation and actuator response limits), resulting in a decreased simulation penetration distance for a given initial velocity. However there still exists some error due to the *required* penetration distance (due to the wall dynamic model where force is a function of penetration distance) for prior rigid body contact simulations in VR applications. In a tele-manipulation application, the penetration distance error can be devastating. If the robotic gripper fingers are rigid and the grasped object is rigid, the simulation penetration distance given by the operator finger over-travel, will result in very high forces of contact between the slave fingers and the object. This may result in damage to either the robotic hand, or the object being grasped, and thus present tele-manipulation systems require a slow grasp speed. The reduced speed may be imposed by the tele-manipulation control system or controlled by the operator.

3.3 Contact Simulation of Proposed Haptic Display

Finally we consider a dynamic model of the proposed DECAFF de-coupled actuator under position control paradigm, as shown in FIG. 4. Because the haptic display actuator is not coupled to the operator, and the position of the contact drum is initially controlled to maintain a position, rather than to apply a force, the simulation position is constant during the contact phase. Also because the distance *before* contact is used to control the contact drum position, the time delays of EQ. (11) are greatly reduced. In mathematical terms,

$$x_s\,(t_1) = x_s\,(t_2) \qquad (16)$$

For the simulation position change of zero, the force during contact F(t), is a function only of the finger mass, spring rate, damping, and position, which is an exact match of the controlling parameters during real contact with a real wall. Thus, the highly transient force experienced by the operator, will be extremely close to that of the real experience, and certainly much more accurate than that possible with the traditional modeling of haptic sensations while contacting virtual walls.

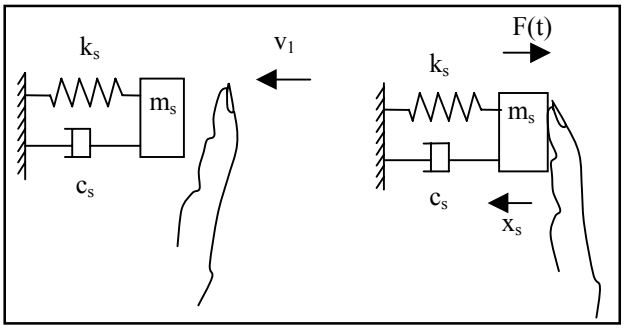

Figure 4 - Finger Contact Simulated Wall (Proposed System)

While the initial contact control is by position, forces of the slave hand (in a tele-manipulation application) are still measured. Once the force values return to a near steady-state magnitude, position control is disabled, and force control is established, permitting accurate representation of both the initial contact with the object, and subsequent force controlled manipulation of the object. In VR simulations, the position control is maintained when interacting with rigid bodies, while force control is used when interacting with deformable bodies, permitting accurate simulations for both types of bodies.

4. Generalization to Multi-Degree of Freedom Systems

Following the method of Ellis et.al. (1997), the above models can be represented by lagrangian equations of motion, yielding solutions for forces at discrete time steps. Although the method presented here follows that of the Ellis paper, two important distinctions are made in the present analysis:

(1) The forces due to damping and spring deflection in the following analysis are not ignored or assumed to be zero.

(2) Both the human finger and haptic interface mass, spring and damping are included in the present model.

The lagrangian formulation of EQ. (2) is given by replacing linear displacement, velocity, and acceleration with spatial generalized coordinates as follows:

$$F(t) = mq''(t) - cq'(t) - kq(t) \qquad (17)$$

This equation can be analyzed term by term, as was done for the linear displacement models, applying boundary conditions of $q(t_1) = 0$, $q'(t_2) = 0$, and $q''(t_2) = 0$. When this is done, we obtain the same conclusions of the real finger real wall model above, in that the final steady state force is small, and the kinetic energy of the finger in motion before contact is primarily dissipated through internal finger damping. If we further evaluate the equation of motion to determine impulse and energy we can describe the motion as follows:

$$q'(t_1) = \int q''(t)\, dt = 1/m \int F(t)\, dt + 1/m \int (cq'(t) + kq(t))\, dt \qquad (18)$$

$$q(t_2) = \int q'(t)\, dt \qquad (19)$$

for limits of integration from t_1 to t_2. Defining shorthand for impulse, damping, and potential

$$\text{Impulse} = I(t_2) = \int F(t)\, dt \qquad (20a)$$

$$\text{Damping} = C(t_2) = \int c\, q'(t)\, dt \qquad (20b)$$

$$\text{Potential} = K(t_2) = \int k\, q(t)\, dt \qquad (20c)$$

We can rewrite EQ. (18) as:

$$q'(t_1) = (1/m)\,(I(t_1) + C(t_1) + K(t_1)) \qquad (21)$$

Noting that we have deviated slightly from that shorthand notation of Ellis by defining separately the damping and potential terms, since we will not be assuming these terms to be zero, we can evaluate the kinetic energy at time t_1 as:

$$E(t_1) = (1/2)\, m\, q'(t_1)^2 = (1/2m)[I(t_1)^2 + C(t_1)^2 + K(t_1)^2$$
$$+ 2\, I(t_1)C(t_1) + 2I(t_1)\, K(t_1) + 2C(t_1)\, K(t_1)] \qquad (22)$$

From which we can conclude as did Ellis, that errors in estimating the impulse term magnify the apparent energy quadratically. However, because damping and potential terms are also considered, we can comment on the quadratic effect of errors in these terms in the energy transfer. To account for real human fingers (or hand) and haptic interfaces which are multi-degree of freedom mechanisms, the lagrangian model can be further generalized as a vector form of EQ. (17):

$$\mathbf{F} = \mathbf{M}(\mathbf{q})\,\mathbf{q}'' + \mathbf{C}(\mathbf{q}, \mathbf{q}')\,\mathbf{q}' + \mathbf{P}(\mathbf{q}) \qquad (23)$$

Where **M** is the mass matrix, **q** is the vector of position variables, **C (q, q')** is the vector of damping forces, and **P (q)** is the vector of potential terms. The energy values are found by integrating the vector form of EQ. (18), where division by m is replaced by multiplication by the inverse of the mass matrix **M**. The quadratic relationship will still hold, subject to the position dependent mass matrix.

From the above analysis we can conclude that force and energy transfer errors are largely attributable to the required penetration distance in the simulated or virtual wall. These errors are also caused by the time delay between the time the force is displayed and the time at which the position data used in force calculation was measured. This effect causes a deeper penetration into the virtual wall, of a magnitude proportionate to the velocity at initial wall contact. Further the delay results in a force to remain applied to the operator after the finger has retracted from the virtual wall boundary. The results of each of these factors are simulated in the following section.

5. Simulation of Results

Equations (2) through (15) can be better understood by examination of a sample case of "typical" finger contacting a wall trajectory, and determining the resulting force vs. time F(t) response. Then equations (16) through (23) will be apparent as applications of the simulations presented in this section. It should be noted that the selection of a typical position vs. time x(t) operator input is quite arbitrary, since this is controlled by the human operator, and thus is subject to high variability between operators and for the same operator on different occasions. Although the x(t) is controlled by the operator and thus likely to be variable, one can make some reasonable assumptions about the trajectory of the finger while in contact with a real wall:

(1) The starting point of x = 0, defined as initial contact position, occurs at time t_1.

(2) At time t_2, the position x has reached a steady state value, indicative of constant (approximately) grasp force while resting the finger against an object.

(3) Between time t_1 and t_2, the position x remains positive, indicating continuous contact between the finger and object.

Subject to the above conditions, an assumed x(t) is created, and differentiated, to yield x'(t), and x"(t). These values along with an assumed k_f = 200 N/m and c_f = 6 N s/m are used to compute F(t), for the cases of real wall contact and simulation wall contact of traditional virtual wall models. The x(t) for traditional wall models is assumed to contain an additional magnitude of the simulation object penetration (x_S). The force F(t) for traditional wall models is presented to lag the position function by a fixed time dt, indicating the delay in force display after initial contact. Plots for the cases of interest are shown in FIG. 5. The units of x are millimeters, while those of F(t) are Newtons. The abscissa axis indicates time in milliseconds. The force plots of FIG. 5a through FIG. 5f are based on the assumption that there is a high virtual damping and spring constant such that the c_{eq} and k_{eq} are approximated by c_f and k_f respectively. The first simulation is that of a real finger contacting a real wall given in FIG. 5a. FIG. 5b shows the simulation position and force that would result if a traditional virtual wall simulation could be performed without time delays in force output. Note that the simulation position includes a wall penetration x_s and a finger deformation x_f. It should be clear from the plot that the steady state force while in contact with the wall is higher for the simulation due to the wall penetration. FIG. 5c presents a force plot that includes the effect of wall penetration and a total time delay of 40 milliseconds, which would be present for a system operating at 25 Hz. In FIG. 5d, a force response is given for a simulation that only includes a delay of 40 milliseconds and no effect of wall penetration. The force data presented here are calculated from the real wall position data and force equation, except that each force data point is based on position, velocity, and acceleration that occurred 40 ms prior to the force time. One observation from this figure is that the delay results in a force being applied to the operator after contact with the object has been lost. The effect of only the virtual wall penetration distance and no delay effect is shown in FIG. 5e. Here the force experienced by the operator demonstrates an error of excess magnitude, and in duration extending beyond contact. Both of the effects of FIGS. 5d and 5e, shown together in FIG. 5c, would likely lead to a "lively" wall perception for the operator. A simulation of the problem of instability between the operator and a haptic interface is shown in FIG. 5f. Here the position of the simulation has been modeled so as to include an operator's response to the prior force output, as might occur when a high magnitude force is applied to the operator's finger. This is done by subtracting the force of the previous time step (multiplied by a constant) from the x_{s+f} data. One can see in this figure that the model is truly unstable, with increasing magnitude of both force and position deviations from that which would be felt while interacting with a real wall. The effect of having a simulation spring constant that was not significantly larger than that provided by the operator is shown in the model of FIG.5g. Here it is assumed that k_{eq} is given by 100 N/m, as one would see if the simulation spring constant and the human operator's spring constant were both 200 N/m. It is clear that this too low spring constant in combination with the other simulation effects tends to decrease the magnitude of the steady state force, subject to the assumed finger trajectory. In FIG. 5h, the results of a similar investigation are shown. Here instead of varying the spring constant, the damping constant is varied for the simulation force output. For this study, the simulation damping constant c_s was given a value of 1.2 N s/m, which results in a c_{eq} of 1 N s/m. For a damping coefficient that is too low, we observe that the force rises more slowly, and retains a high value longer after contact is lost than that of the matching $c_{eq} = c_f$ and $k_{eq} = k_f$ simulation.

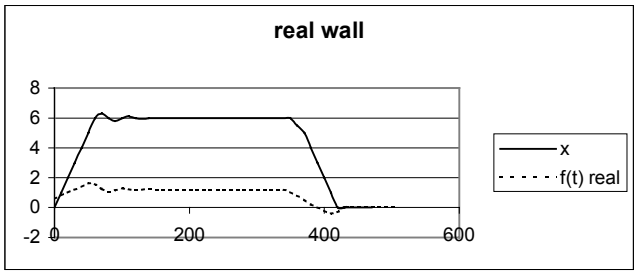

Figure 5a – Real Wall Model Displacement and Force

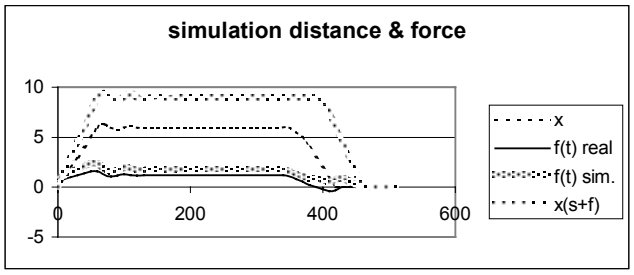

Figure 5b – Simulation and Real Displacement and Force

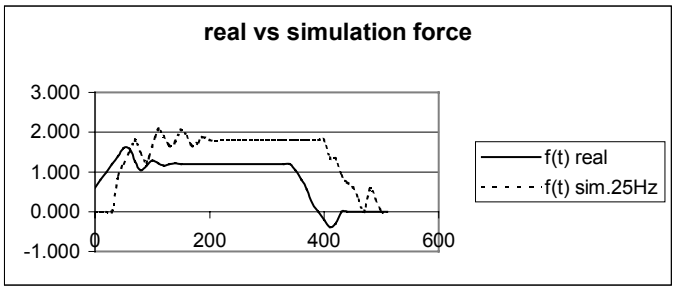

Figure 5c – Simulation and Real Wall Model Force

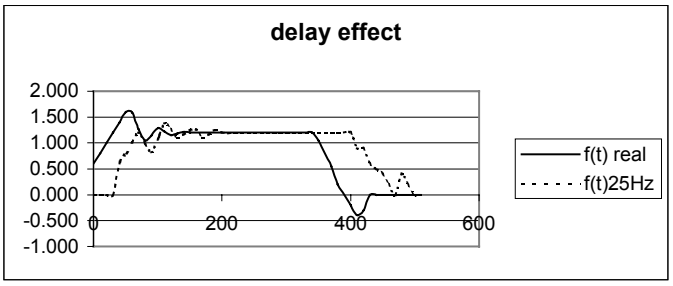

Figure 5d – Simulation and Real Wall Model Force – Effect of Time Delay

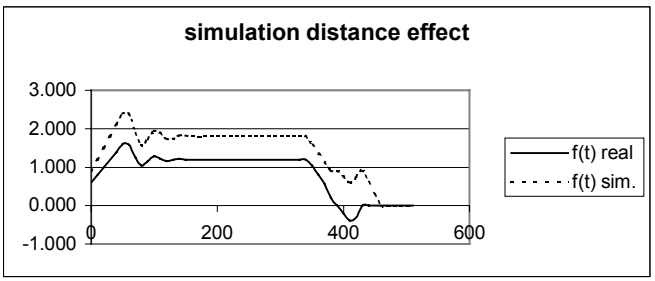

Figure 5e - Simulation and Real Wall Model Force – Effect of Wall Penetration

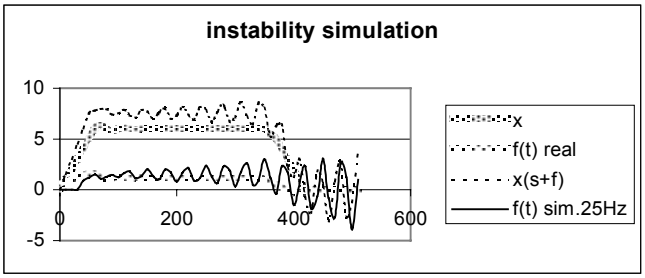

Figure 5f – Simulation and Real Wall Model Force – Instability Model

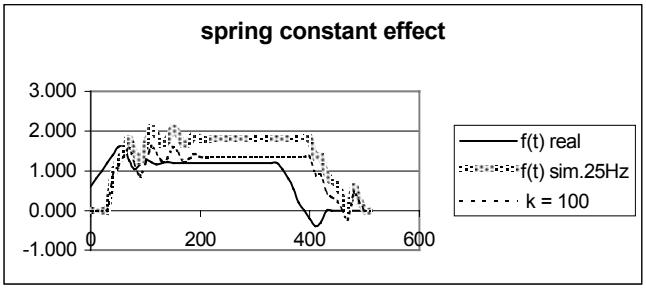

Figure 5g – Simulation and Real Wall Model Force – Spring Constant Effect

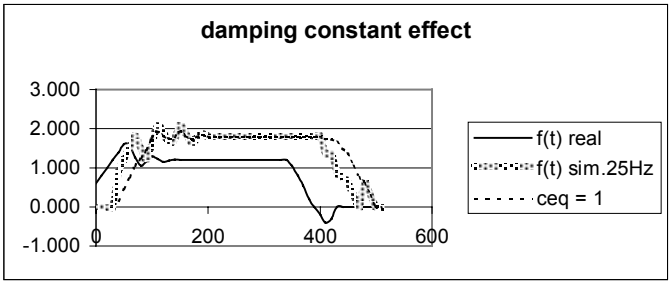

Figure 5h – Simulation and Real Wall Model Force – Damping Constant Effect

6. Conclusions

In this paper a new approach to the design and control of haptic interfaces to specifically address previously reported deficiencies in the haptic display of rigid surfaces has been proposed. Simplified dynamic models of the finger interacting with a real wall, the finger interacting with a traditional haptic interface, and the finger interacting with the proposed de-coupled actuator, feed forward control haptic interface have been presented. By reduction of time delays and elimination of the need for wall penetration in the proposed approach, we can conclude that the new approach will be able to more accurately represent initial contact with rigid objects. Consequently, a method to solve an important problem in the haptic display

research area has been addressed (in theory). This has been done while simultaneously increasing interface transparency and maintaining the desirable property of force controlled display during manipulation, following the initial contact phase. The solution to the problem of representation of initial contact with rigid surfaces as proposed, has an additional expense for both the tele-manipulation and the virtual reality application areas. The expense for VR owing to the fact that additional computation is required to determine the feed forward term (distance to contact) before contact. For the tele-manipulation application, the expense is the addition of a sensing element to determine the distance between the slave finger and any approaching object. For VR applications, the proposed method of determining distance to contact requires a point/solid intersection or line/solid intersection, each of which carries some small computation load. At the present time a complete VR application has not been implemented to verify the precise performance cost of these intersection checks. Because the tele-manipulation application merely requires that measured distance information be directly sent to the haptic controller, without computation, it is anticipated that computation penalties for this application will be minimal.

7. Future Research

In order to verify the proposed systems claims to provide a superior method to display rigid surfaces, formal human experimentation has been planned. The experimentation will include a comparison of the proposed method of haptic display described herein with the traditional directly coupled actuator design and spring-damper wall model traditionally employed. At the time of submission, work is under way as to the specific design and execution of the experimental study. Current work is also under way to implement the system described in this paper into a VR graphical environment, in order to evaluate the computation cost of pre-contact distance calculations.

References

Colgate, J., Grafing, P., Stanley, C., and Schenkel, G., 1993, Implementation of Stiff Virtual Walls in Force Reflecting Interfaces, *Proceedings of Virtual Reality Annual International Symposium,* IEEE Neural Networks Council, Piscataway, NJ, pp. 202-215.

Ellis, R., Sarkar, N., Jenkins, M., 1997, Numerical Methods of the Force Reflection of Contact, *Transactions of the ASME, Journal of Dynamic Systems, Measurement, and Control*, Vol. 119, pp. 768-774.

Hajian, A., and Howe, R., 1994, Identification of the Mechanical Impedance of Human Fingers, *Proceedings of the 1994 ASME Winter Annual Meeting*, DSC-Vol. 55-1, ASME, New York, NY, pp. 319-327.

Karson, S., Srinivasan, M., 1995, Passive Human Grasp Control of an Active Instrumented Object, *Proceedings of the 1995 ASME International Mechanical Engineering Congress and Exposition*, DSC-Vol. 57-2, ASME, New York, NY, pp. 641-647.

Kazerooni, H., 1993, Human Induced Instability in Haptic Interfaces, *Proceedings of the 1993 ASME Winter Annual Meeting*, DSC-Vol. 49, pp 15-27.

Lawrence, D, Salada, M., Lucy, P., and Doughtery, A., 1996, Quantitative Experimental Analysis of Transparency and Stability in Haptic Interfaces, *Proceedings of the 1996 ASME International Mechanical Engineering Congress and Exposition*, DSC-Vol. 58, ASME, New York, NY, pp. 441-449.

Li, Y., 1996, A Sensor Based Robot Transition Control Strategy, *International Journal of Robotics Research*, Vol. 15, No., 2, April 1996, pp. 128-136.

Love, L., and Book, W., 1995, Contact Stability Analysis of Virtual Walls, *Proceedings of the 1995 ASME International Mechanical Engineering Congress and Exposition*, DSC-Vol. 57-2, ASME, New York, NY, pp. 689-694.

Norton, R., 1999, Design of Machinery, An Introduction to the Synthesis and Analysis of Mechanisms and Machines, Second Edn., McGraw-Hill, New York, NY, pp 500-512.

Salcudean, S., Vlaar, T., 1994, On the Emulation of Stiff Walls and Static Friction with a Magnetically Levitated Input/Output Device, *Proceedings of the 1994 ASME Winter Annual Meeting*, DSC-Vol. 55-1, ASME, New York, NY, pp. 303-309.

Springer, S., Gadh, R., 1996, State-of-the-art Virtual Reality Hardware for Computer-aided-design, *Journal of Intelligent Manufacturing*, Volume 7, pages 457-465, December, 1996.

Springer, S., Gadh, R., 1997, Haptic Feedback for Virtual Reality Computer Aided Design, *Presented at the 1996 ASME International Mechanical Engineering Congress and Exposition*, November 1997, Dallas, TX, ASME, New York, NY.

Springer, S., 1998, Force Display Master Interface Device for Teleoperation, U. S. Patent Application S/N 09/195,318.

Springer, S., Ferrier, N, 1999, Design of a Multi-finger Haptic Interface for Teleoperational Grasping, *Presented at the 1999 ASME International Mechanical Engineering Congress and Exposition*, November 1999, Nashville, TN, ASME, New York, NY.